Journal of the Brazilian Society of Mechanical Sciences and Engineering (2021) 43:249
https://doi.org/10.1007/s40430-021-02974-x

TECHNICAL PAPER

Analysis of temperature and surface finish of Inconel 718 during grinding utilizing different grinding wheels

Rodrigo de Souza Ruzzi[1,2] · Raphael Lima de Paiva[1,3] · Alisson Rocha Machado[1,4] · Rosemar Batista da Silva[1]

Received: 25 January 2021 / Accepted: 31 March 2021 / Published online: 11 April 2021
© The Brazilian Society of Mechanical Sciences and Engineering 2021

Abstract
Nickel-based superalloy Inconel 718 is widely used for aeronautical applications, such as blades and discs of aircraft engines, and therefore is generally submitted to a grinding process in order to meet the required surface finish and dimensional accuracy. However, the mechanical and thermal properties of Inconel 718 make it a material with low machinability (difficult-to-machine material). Therefore, the proper selection of abrasives is of high importance, when aiming to improve process efficiency. White aluminum oxide (WA) and green silicon carbide (GC) abrasives are the most common conventional abrasives employed in the grinding of nickel-based superalloys, and their different properties can be decisive when it comes to the success of the process. In this sense, this work sought to evaluate the performance of two conventional abrasives (WA and GC) in the grinding of Inconel 718 with cutting fluid applied with a conventional technique. Five different cutting conditions were tested. Surface finish (Ra and Rz parameters) and cutting region temperature were used to assess grinding performance. The results showed that, compared to WA, grinding with the GC wheel reduced roughness in 14% and 19% for Ra and Rz, respectively, even though this produced higher cutting region temperatures (55% higher in general). However, for more severe cutting conditions (e.g., higher values of radial depth of cut), the characteristic wear mechanism of the GC wheel further increases cutting region temperature, resulting in surface finish deterioration.

Keywords Inconel 718 · Grinding · Conventional abrasives · Surface finish · Grinding temperature

1 Introduction

Nickel-based superalloys are important raw materials for components applied in critical environments (e.g., aerospace and nuclear industries) due to their high-temperature strength, high oxidation resistance and corrosion resistance [1, 2]. Such components usually require tight dimensional tolerances (< 10 µm), low values of surface finish (Ra < 0.5 µm) and a surface integrity free of cracks and tensile stresses. Therefore, the grinding process is generally the first option to meet these requirements [3]. Among various grades of nickel-based superalloys, Inconel 718 stands out, since it corresponds to almost half of all wrought nickel-based alloy production [4, 5]. Furthermore, according to Ezugwu et al. [6], Inconel 718 accounts for about half the weight of aerospace engines, mostly in gas turbine components.

However, the thermal, mechanical and chemical properties which make Inconel 718 suitable for the above-mentioned applications affect its machinability in an adverse manner. Additionally, its low thermal conductivity, high work hardening tendency and chemical affinity to most tool materials further increase the challenge in machining Inconel 718, especially considering high specific energy processes, such as grinding [7]. With respect to the use of conventional abrasives such as alumina (Al_2O_3) and silicon

Technical Editor: Lincoln Cardoso Brandao.

✉ Rodrigo de Souza Ruzzi
rodruzzi@gmail.com

1 School of Mechanical Engineering, Federal University of Uberlandia (UFU), Av. João N. de Ávila, 2121, Uberlândia, Minas Gerais, Brazil

2 Department of Mechanical Engineering, Ingá University Center (UNINGÁ), Rod. PR-317, 6114, Parque Industrial 200, Maringá, Paraná 87035-510, Brazil

3 School of Mechanical Engineering, Federal University of Piauí, Campus Univ. Min. Petrônio Portella - Ininga, Teresina, Piauí, Brazil

4 Mechanical Engineering Graduate Program, Pontifícia Universidade Católica do Paraná – PUC-PR, Curitiba, Paraná CEP 80215-901, Brazil

carbide (SiC), the grinding of Inconel 718 is even more challenging, since these abrasive grits present low thermal conductivity, especially at high temperatures, thereby contributing to increased heat accumulation and the development of high temperatures at the contact zone [8]. In this sense, depending on temperature levels and time of action, the integrity of the workpiece surface can be compromised (e.g., grinding burn, surface finish deterioration and surface defects), and the grinding wheel wear rate critically increased [9, 10].

The use of superabrasives, as in diamond and cubic boron nitride (cBN), can be an alternative due to their higher thermal conductivity, which contributes toward reducing the heat partition conducted into the workpiece. In this way, Xi et al. [11] conducted a grinding experiment comparing both superabrasives grits and concluded that higher hardness and thermal conductivity contribute to reducing the occurrence of thermal damage, even at high material removal rates. Therefore, due to the aforementioned, superabrasive wheels are preferred for grinding difficult-to-cut materials, such as Inconel 718. However, the use of conventional abrasive wheels is still suitable for grinding this class of material, as these are less expensive and more flexible regarding the dressing operation, thereby favoring the manufacturing of complex grinding wheel forms, which play an important role, especially in aerospace applications [12–14]. Besides the use of cBN wheels, other alternatives, such as the use of ultrasonic vibration-assisted grinding (UVAG) or the application of nanofluids through minimum quantity lubrication (MQL) technique, can be used in order to reduce cutting forces and improve surface quality when grinding Inconel 718 with alumina wheel [15–17].

White aluminum oxide (WA) and green silicon carbide (GC) are the most common conventional abrasives employed in grinding. The former presents lower hardness and superior fracture toughness in comparison with the latter, and as such results in a lower friability, which is the tendency of a material to break up into smaller fragments under pressure [18, 19]. In this sense, considering the same grinding conditions in terms of grit size, bond material and cutting parameters, WA abrasive grits are more likely to present, in theory, total breakout or macro-fracture, due to its higher toughness in comparison with GC grits. However, noteworthy here is that other factors, such as chemical affinity between abrasive and workpiece material, have an intense effect on the abrasive grit wear mechanism [14].

In addition to hardness and fracture toughness resistance, WA and GC abrasive grits present different thermal properties. According to Rowe [20], thermal conductivity at room temperature (RT) of WA and GC are 35 $Wm^{-1}\ K^{-1}$ and 100 $Wm^{-1}\ K^{-1}$, respectively. At high temperatures, 727 °C for instance, these values reduce to about 7 $Wm^{-1}\ K^{-1}$ and 60 $Wm^{-1}\ K^{-1}$ for WA and GC, respectively [21]. In terms of thermal expansion coefficients (α), GC presents lower dimensions variation with temperature: $\alpha = 4.3–4.8\ °C^{-1} \times 10^{-6}$ for GC and $\alpha = 7.2–8.8\ °C^{-1} \times 10^{-6}$ for WA [22]. A summary of major thermal–mechanical properties of both WA and GC abrasive grits is shown in Table 1.

Regarding Al_2O_3 abrasive grits, note should be made that the different classes may present a different performance in grinding nickel-based superalloys. To this end, Li et al. [23] investigated the grinding forces, grinding temperature, surface quality and tool wear in the creep feed grinding of powder metallurgy nickel-based superalloy FGH96 with different alumina wheels (brown alumina—BA, and microcrystalline alumina—MA). The findings showed that both abrasive wheels promoted the similar results in terms of grinding forces, surface finish and wheel wear. Grinding with the MA wheel allowed for the use of a higher material removal rate without grinding burn, indicating a slightly higher grinding efficiency in comparison with the BA wheel. According to the authors, the self-sharpening characteristic of the MA abrasive wheel contributes toward reducing heat generation at the contact zone.

With respect to the grinding of Inconel 718, using conventional abrasive grinding wheels, Huddedar et al. [24] investigated surface finish (Ra parameter) of the workpiece after grinding under various cooling environments and three different Al_2O_3 grinding wheel grit sizes (mesh of #60, #120 and #220). They also varied workspeed (8 m/min, 10 m/min and 12 m/min) and radial depth of cut (50 µm, 100 µm and 150 µm). The findings showed that the Ra values increased with the increase of grit size and radial depth of cut (a_e), while workspeed (v_w) did not affect this output parameter. The values of Ra achieved were in the range of 0.20–1.2 µm.

Research conducted by Mahata et al. [2] also used an Al_2O_3 grinding wheel (designation of AA60K5V8) in their

Table 1 Major thermal and mechanical properties of WA and GC conventional abrasive grains material [18, 20–22]

Properties	WA	GC
Hardness Knoop (HK)	2000–2160	2400–3000
Relative toughness (%)	15	3
Thermal conductivity at room temperature ($Wm^{-1}\ K^{-1}$)	35	100
Thermal conductivity at 1000 K (727 °C) ($Wm^{-1}\ K^{-1}$)	7	60
Thermal expansion ($°C^{-1} \times 10^{-6}$)	7.2–8.8	4.3–4.8

work during grinding of Inconel 718 under different cooling–lubrication conditions, and radial depth of cut (a_e) of 10 µm, wheel speed (v_s) of 30 m/s and workspeed (v_w) of 14 m/min. In terms of surface finish, the authors recorded Ra values in the range varying from 0.97 to 1.26 µm, and Rz between 5.51 and 6.68 µm. From these results one notes that, even when grinding at a low radial depth of cut (10 µm), the values for the surface finish are considered high in comparison with those generally observed in the grinding of hardened steel under similar cutting conditions, such as those reported by Tawakoli et al. [25].

Collaborators in Sinha et al. [10] investigated grinding forces and surface finish (Ra parameter) in the grinding of Inconel 718 under different cooling–lubrication conditions (dry, wet, MQL and liquid nitrogen—LN_2). The authors employed a vitrified bonded white alumina wheel, with a designation of A60K5V. Grinding parameters were also varied in terms of v_s (10 m/s, 15 m/s and 20 m/s), v_w (3 m/min, 9 m/min and 15 m/min) and a_e (10 µm, 15 µm and 20 µm). The authors reported that the Ra parameter varied in the range from 0.35 to 0.55 µm. Furthermore, their findings showed that Ra decreased for higher values of wheel speed (v_s) and increased with v_w and a_e, irrespective of the cooling–lubrication condition. Dry grinding presented low values of Ra, which was attributed to intense rubbing, a result of wear flat that leads to grinding wheel dulling. This was attenuated by using cutting fluid, especially for wet (flood technique) and LN_2 conditions. Noteworthy here is that the authors observed surface oxidation after grinding with all cooling–lubrication conditions, except when grinding with LN_2, which increased sharply the process of heat removal from the contact zone.

The study by De Oliveira et al. [26] carried out an experimental investigation in the grinding of Inconel 718 using the conventional green silicon carbide grinding wheel (designation of 39C60KVK) under various cooling–lubrication conditions: dry, flood, MQL and MQL with multilayer graphene platelets dispersed in an eco-friendly cutting fluid. Different values of a_e were tested: 20 µm and 40 µm. Although the findings showed low Ra roughness (< 0.42 µm), the authors observed the occurrence of microcracks on all ground surfaces, irrespective of the grinding condition.

In a more recent work, De Oliveira et al. [7] carried out a study to evaluate the grindability of Inconel 718 using a conventional white aluminum oxide grinding wheel (designation of AA60K6V). During the study, different coolant delivery techniques (flood and MQL) were tested. The cutting parameters used by the authors were: $v_s = 35$ m/s, $v_w = 10$ m/min and three different values of a_e (10 µm, 20 µm and 30 µm). They reported surface finish (Ra parameter) between 0.15 and 0.43 µm. Furthermore, the results showed that machining with the MQL technique generated higher values of Ra and poorer surface texture quality in comparison with the flood technique, which was attributed as possessing a lower cooling capacity than the MQL technique. The authors also pointed out that the chip formation mechanism, during grinding of Inconel 718 with conventional abrasives, can be unpredictable.

Research performed by Tso [27] studied the grinding of Inconel 718 with different types of abrasive grinding wheels: WA (WA46K8V), GC (GC60J8V) and cBN (CBN100P75V). The author employed the following cutting parameters for the grinding experiments: $v_s = 11$–22 m/s, $v_w = 2$–5 m/min and $a_e = 5$–15 µm. The results showed that grinding with the cBN wheel produced a better surface finish (low values of Ra) in comparison with grinding with GC and WA wheels. Furthermore, surface roughness increased for low values of v_s and increased with v_w and a_e. The author concluded that the cBN grinding wheel is the most suitable for the grinding of Inconel 718, irrespective of its machinability index (grinding force, surface finish, dimensional accuracy and grinding wheel wear). Cost factor was not considered by the author.

In another similar work, Tso [28] investigated the chip types in the grinding of Inconel 718 with the same grinding wheels used in a previous study by the author [27]. The findings showed that both the abrasive type and cutting environment (dry or flood) influenced chip type, which in turn affected the workpiece surface finish. In general, cBN grinding wheels promoted the formation of chip types that were associated with a better surface finish. The ripping chip type, associated with the worst surface finish, was observed only when grinding with the GC wheel, which experienced severe attrition wear, thereby resulting in high grinding temperature and even chip adhesion to the surface of the workpiece.

The corroborators in Sinha et al. [8] conducted an experimental study in the grinding of Inconel 718, while comparing conventional WA and GC grinding wheels with designation of WA60K5V and GC60K5V, respectively. The grinding experiments were carried out for the dry condition (no application of cutting fluid). Workpiece surface integrity was assessed in terms of EDX, XRD, XPS, SEM images, surface finish and micro-hardness. Grinding forces and coefficient of friction were also evaluated. The cutting parameters employed by the authors were: wheel speed (v_s) of 10 m/s and 20 m/s, v_w of 3 m/min and 15 m/min, and a_e of 5 µm and 15 µm. The authors noted that all surfaces ground using the GC wheel presented clear burning marks, which was attributed to oxide layer formation and phase transformation, due to the accumulation of heat over the workpiece surface. Additionally, the findings showed that grinding with the WA wheel improved surface finishing (lower values of Ra) in comparison with GC wheels, with no visible burning marks on the ground surface. According to the authors, grinding Inconel 718 with CG wheels under dry conditions

Table 2 Chemical composition of Inconel 718 alloy

Font	Element	Ni	Cr	Fe	Nb	Mo	Ti	Al	C
EDS map analysis	%	52.2	19.2	17.8	6.71	2.65	1.25	–	–

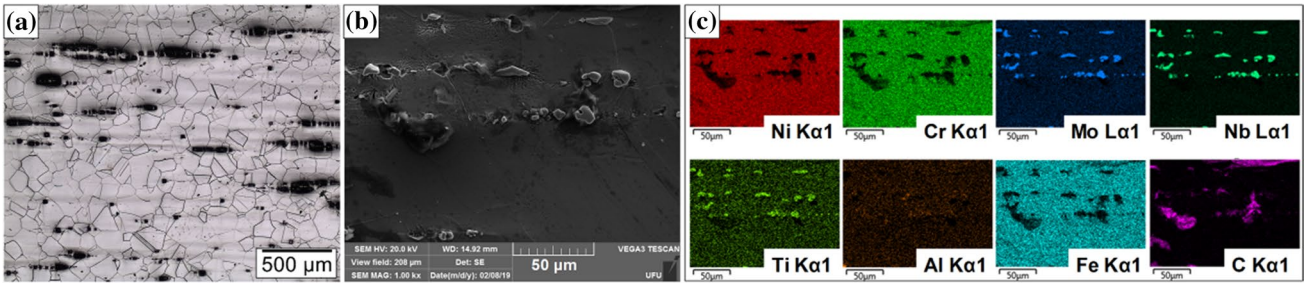

Fig. 1 Metallographic analysis of Inconel 718 prior to the grinding process. **a** Optical microscopy of the etched sample showing grain and twin boundaries (etched with Kallings 2); **b** SEM image with secondary electron, and **c** EDS mapping analysis identifying the respective element

resulted in severe abrasive grain-workpiece rubbing due to accelerated wear of GC grits, which increases cutting temperature and favors the chemical reaction between the abrasive grains and workpiece, thereby resulting in intense chip adhesion on the ground surface. Furthermore, the authors recorded a lower coefficient of friction as well as lower tangential forces during grinding with WA wheels.

Noteworthy here is that an important output parameter from grinding is the cutting region temperature reached during the process, since this can be associated with the occurrence of thermal damage on the workpiece. In this way, different methodologies of temperature measurement during grinding are reported in the literature. Kuriyagawa et al. [29] present a methodology for grinding temperature measurement within the contact arc between the grinding wheel and the workpiece in the creep-feed grinding of cermet Ti(C,N) alloy. The same methodology was called double pole thermocouple and employed by Batako et al. [30]. Another methodology, typically employed for reading grinding temperature measurement, consists of inserting a thermocouple in a blind hole at a specific distance beneath the grinding surface, as employed by Awale et al. [31] and Hadad et al. [12].

In this context, there is a lack of more recent papers that focus on the comparison between different conventional abrasive grain types in the grinding of Inconel 718, especially under wet grinding conditions (cutting fluid applied with the flood technique) and cutting temperature measurements. Therefore, this work sought to evaluate the surface finish and cutting region temperature during the wet grinding of Inconel 718 using conventional WA and GC grinding wheels with different values of radial depth of cut (a_e).

Table 3 Physical properties of Inconel 718 alloy [35]

Melting range (°C)	Density (g/cm^3)	Specific heat (J/kg.°C)	Coefficient of expansion (µm/m·K)	Thermal conductivity (W/m·K)
1260–1336	8.19	435	13	11.4

2 Materials and methods

2.1 Material

The nickel-based Inconel 718 alloy (513 ± 10 HV$_{0.5}$) was supplied by Villares Metals S.A. under the trade name Inconel VAT718A®. The samples were supplied as aged, with the chemical composition and microstructure shown in Table 2 and in Fig. 1, respectively. An optical microscope (Olympus, BX51 model), with a magnification of 500×, and a scanning electron microscopy (SEM) (TESCAN, VEGA 3 model), with magnification of 2000×, equipped with energy-dispersive X-ray spectroscopy (EDS) mapping from Oxford Instruments were used to analyze the samples. The EDS analysis was performed in the region shown in Fig. 1b and the resulted color map is presented in Fig. 1c.

After etching the Inconel 718 with Kallings 2 (Fig. 1a), the metallographic analysis revealed the grain and twin boundary characteristics of the material. Hard carbide phases with a coherent orientation (originating from the aging process) are also noted [32, 33]. From the EDS map (Fig. 1c), the composition of the oriented precipitated presented in Fig. 1b is seen, which consists mainly of niobium (Nb), molybdenum (Mo) and titanium (Ti), surrounded by the gamma matrix (γ-phase) [33, 34],

Table 4 Mechanical properties of Inconel 718 alloy [36]

Temperature (°C)	Tensile strength (MPa)	Yield strength (MPa)	Elongation (%)
21	1430	1190	21
540	1280	1060	18
650	1230	1020	19
760	950	740	25
870	340	330	88

mainly composed of nickel (Ni) chromium (Cr) and Iron (Fe). The physical and mechanical properties of Inconel 718 are presented, according to the literature [35, 36], in Tables 3 and 4, respectively. From Table 4, one notes that Inconel 718 alloy possesses the characteristic of retaining its resistance (tensile and yield strength) at high temperatures. The workpieces were prepared for the grinding tests with dimensions of 35 mm × 40 mm × 7 mm (length × height × width).

2.2 Experimental procedure

Grinding experiments were conducted on a peripheral surface grinding machine P36, manufactured by MELLO, with a spindle motor of 2.25 kW nominal power and 2400 rpm of spindle speed. Two different conventional grinding wheels manufactured by Norton Saint-Gobain were tested: a white alumina oxide (WA) and a green silicon carbide (GC). Both grinding wheels present abrasive grit size of mesh #60. The grinding wheels designations are 38A60K6V and 39C60K6V for WA and GC, respectively. Both models have an external diameter of 250 mm.

The cutting parameters employed in this study were: wheel speed (v_s) of 31 m/s, workspeed (v_w) of 7.5 m/min, effective wheel width (b) of 7 mm and four different values of radial depth of cut (a_e): 10 µm, 20 µm, 30 µm, 40 µm and 50 µm. The specific material removal rates tested were therefore 1.25 $mm^3 \cdot (mm \cdot s)^{-1}$, 2.50 $mm^3 \cdot (mm \cdot s)^{-1}$, 3.75 $mm^3 \cdot (mm \cdot s)^{-1}$, 5.00 $mm^3 \cdot (mm \cdot s)^{-1}$ and 6.25 $mm^3 \cdot (mm \cdot s)^{-1}$. These cutting conditions were chosen based on previous studies carried out on the surface grinding of Inconel 718 [7–9, 37]. The grinding wheel topography was prepared before each grinding experiment, using a single point dresser with an effective width of the dressing tool (b_d) of 0.30 mm, and a dressing speed (v_{sd}) of 180 mm/min. These dressing parameters resulted in an overlap ratio (U_d) equal to 4. All grinding tests were replicated twice (three tests for each condition).

The experiments were conducted by using the conventional cooling–lubrication technique (flood) with a flow rate of 11 L/min. The nozzle was positioned, in tangential fashion, to deliver the cutting fluid at the contact zone onto the grinding wheel. The cutting fluid employed was the synthetic GRINDEX 10, manufactured by Blaser Swisslube, applied at a concentration of 5% (1:20 oil-in-water dilution). The setup used for the grinding experiments is shown in Fig. 2.

The output parameters analyzed in the present work were the surface roughness of machined surfaces (Ra and Rz parameters) and the cutting region temperature during grinding. Surface roughness was measured using a portable surface tester SJ-201P, manufactured by Mitutoyo. Three different measurements on the machined surface were taken for each grinding test, perpendicular to the grinding direction. The average and standard deviation were selected for analysis. A cutoff of 0.8 mm and 4.0 mm evaluation length was used in accordance with ISO 4288:1996 [38].

The cutting region temperature was measured by using the double-pole thermocouples methodology [29, 30]. This methodology consists of placing together the wires of nickel–chromium and nickel–alumel (K-type thermocouple) separated by a mica sheet and isolated from the workpiece by mica sheets and pressed between two samples cut in half. With the grinding wheel engaged at the cutting zone, the thermocouple wires formed the hot junction, measuring the cutting region temperature. A thermal data acquisition system AGILENT 349780A from KEYSIGHT was used. Figure 3 shows a schematic view of the temperature measurement methodology employed in this work. For the temperature measurements, each grinding condition was replicated twice, and an example of thermocouple K-type measurement, for the grinding condition with WA wheel and $a_e = 10$ µm, is shown in Fig. 4. Average and standard deviation were used for analysis.

Analysis of variance (ANOVA) was performed for both surface roughness and cutting region temperature results,

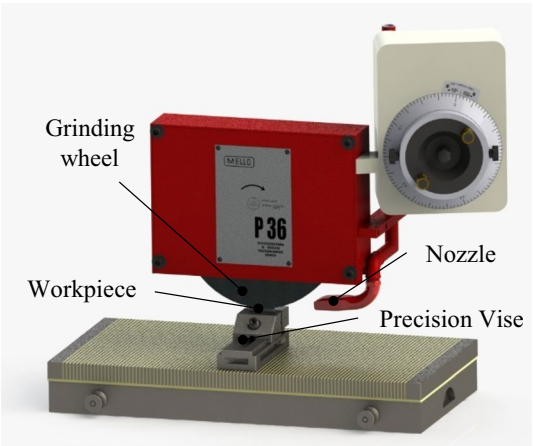

Fig. 2 Schematic illustration of the setup used for the grinding experiments

in order to increase statistical reliability of the results presented in this work, while also verifying whether abrasive type and radial depth of cut were statistically significant considering the conditions tested in this work. All grinding

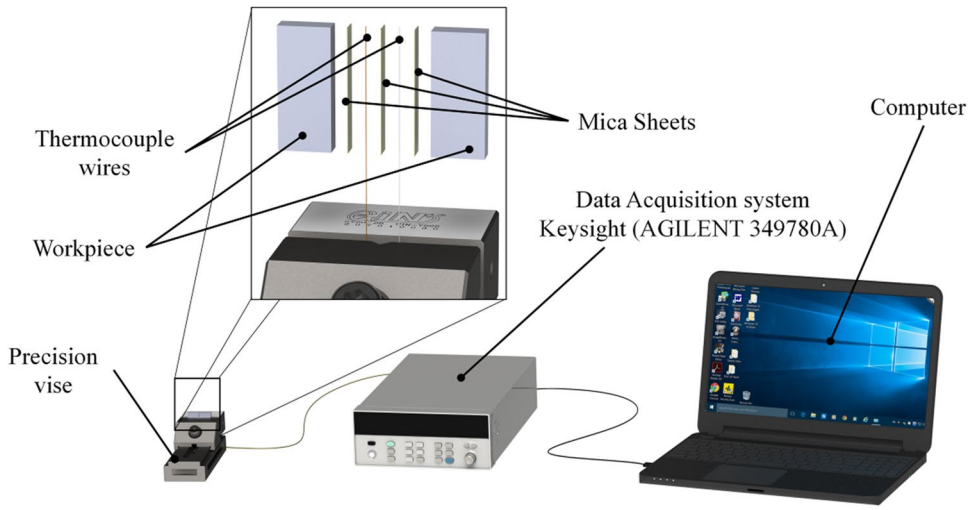

Fig. 3 Illustrative scheme of temperature measurement methodology

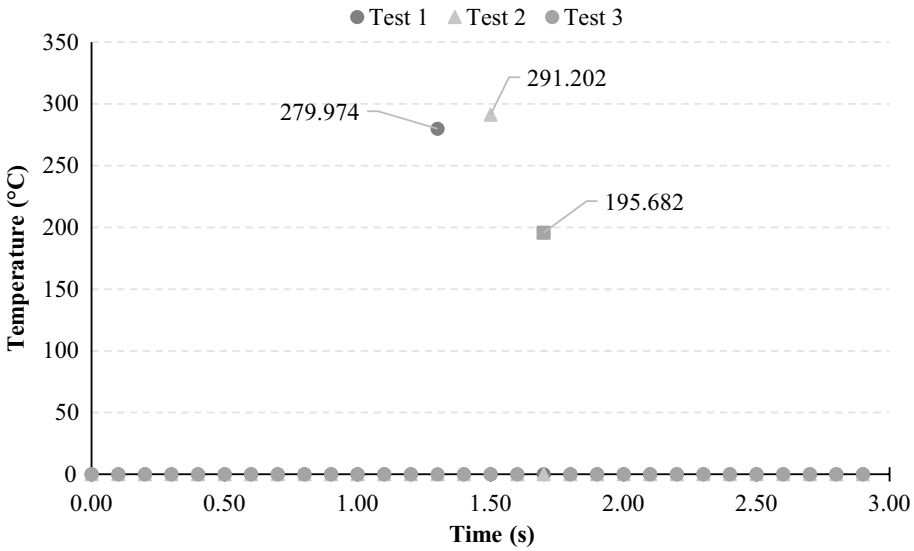

Fig. 4 Temperature measurements for the grinding condition with WA wheel and $a_e = 10$ µm

Table 5 Grinding conditions and output parameters

Grinding wheel	Al_2O_3—38A60K6V—Ø 250 mm (WA)
	SiC—39C60K6V—Ø 250 mm (GC)
Workpiece material	Inconel 718 (42 HRC)—35 mm × 40 mm × 7 mm
Wheel speed (v_s)—m/s	31
Workspeed (v_w)—m/min	7.5
Effective wheel width (b)—mm	7
Radial depth of cut (a_e)—µm	10, 20, 30, 40 and 50
Cooling–lubrication technique	Flood – 11 L/min
Cutting fluid	Synthetic Grindex 10
	5% concentration (1:19 oil in water dilution)
Dressing conditions	Single point dresser, $b_d = 0.3$ mm, $v_{sd} = 180$ mm/min, $U_d = 4$
Output parameters	Surface finish (Ra and Rz parameters)
	Cutting region temperature

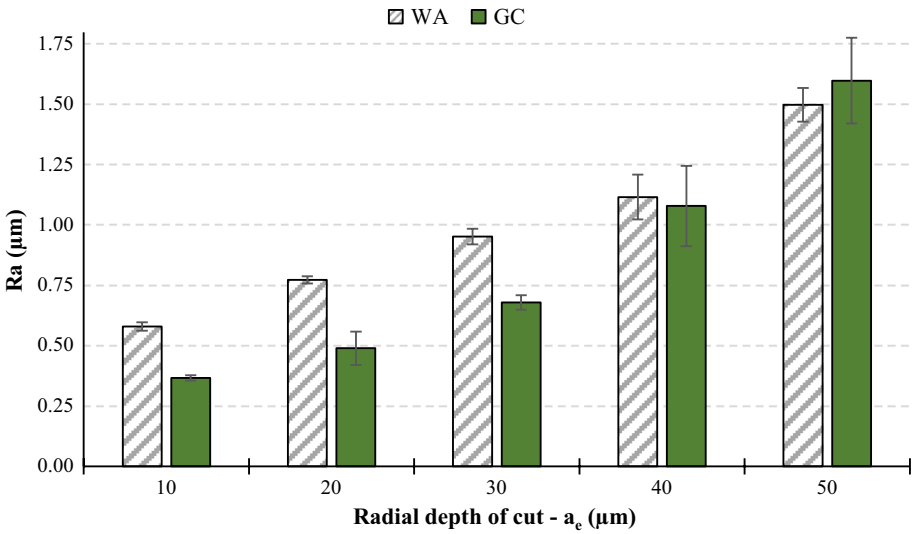

Fig. 5 Roughness Ra of Inconel 718 after grinding with WA and GC grinding wheels as a function of radial depth of cut (a_e)

Table 6 Analysis of variance (ANOVA) for Ra parameter results

Source	DoF	SS	MS	*F*-value	*P*-value
Main effects					
(1) Abrasive type	1	0.1498	0.14981	18.67	0.000
(2) a_e (µm)	4	4.3311	1.08277	134.95	0.000
2-Factor interaction					
(1)*(2) Abrasive type vs. a_e (µm)	4	0.1680	0.04199	5.23	0.005
Error	20	0.1605	0.00802		
Total	29	4.8093			

conditions and output parameters are summarized in Table 5.

3 Experimental results and discussion

3.1 Surface finish: Ra and Rz parameters

The average values of the Ra parameter, after grinding with both grinding wheels tested in this work, are shown in Fig. 5 as a function of radial depth of cut (a_e). From Fig. 5, one notes that all the Ra values are between 0.37 and 1.60 µm, which sits in the range for surface roughness (Ra parameter), as is commonly reported in the literature for the semifinishing grinding process (0.1–1.6 µm) [39]. Furthermore, one notes that grinding with the GC grinding wheel outperformed WA in terms of surface finish, with the exception of the most severe grinding condition (a_e = 50 µm). Finally, one notes from Fig. 5 that the Ra parameter increased with radial depth of cut for both abrasive types tested in this study.

The ANOVA result for the Ra parameter is shown in Table 6, where DoF, SS and MS are the degree of freedom, sum square and mean square, respectively. The *F* value is the relationship between factor and error mean square (MS), where the *P* value is obtained through *F* distribution curves. One notes from Table 6 that abrasive type, radial depth of cut and their interaction presented a *P*-value lower than 0.05. Therefore, considering a confidence interval of 95%, all the factors investigated in this study are statistically significant to the Ra parameter results, including their interaction. Main effects and interaction graphs are shown in Fig. 6.

From Fig. 6a, one notes that grinding Inconel 718 with the GC grinding wheel contributed toward reducing the Ra parameter on the ground surface in the range of 14% in comparison with the WA grinding wheel. This result challenges

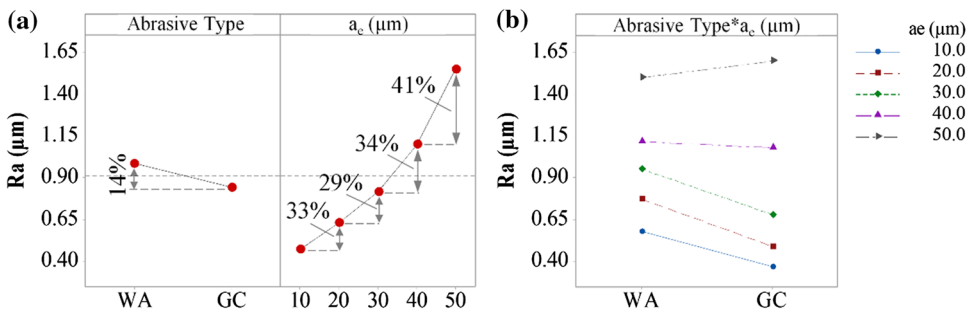

Fig. 6 Main effects and interaction graphs for the Ra parameter results

the findings of Sinha et al. [8], who observed lower values of Ra roughness for Inconel 718 after grinding with the WA wheel, when compared to GC. However, emphasis is here placed on the fact that the grinding experiments carried out by the authors were done so without the application of cutting fluid (dry grinding), this resulted in visible burning marks on the ground surfaces when using the GC wheel. Such grinding burn indicates the development of high temperatures at the contact zone due to heat accumulation, which increases wheel wear and favors chemical reactions between SiC grits and the workpiece. This results in material re-adhesion onto the machined surface, thereby increasing roughness Ra.

The grinding conditions used in this current work, on the other hand, included the application of cutting fluid using the conventional technique (flood—wet grinding), which therefore strongly increases heat dissipation at the cutting zone in comparison with dry grinding. In addition to the cooling action of the cutting fluid, the lubrication effect can also be taken into consideration. Therefore, the application of the cutting fluid brings about remarkable changes to the tribological condition at contact zone, when compared to dry grinding. Both effects of the cutting fluid (cooling and lubrication) contribute to better temperature control, thereby preventing, or at least minimizing, abrasive grit wear and material re-adhesion onto ground surface. Therefore, when considering unburnt ground surfaces, the heightened thermal properties of the GC wheel in comparison with the WA (higher heat conductivity and lower thermal expansion [20]) further improves heat dissipation at the contact zone. This attenuates workpiece deflection and abrasive grit wear, thereby positively affecting surface finish (lower values of Ra).

However, it is known that heat generation increases with increased material removal rate [18]. In this sense, considering the same cooling–lubrication condition, the heat dissipation and lubrication may not be sufficient, when grinding severity is increased to higher limits (e.g., higher values of a_e). In this scenario, similar to dry grinding, the higher heat accumulation then favors chemical reaction(s) between the GC and the workpiece surface, as observed by Sinha et al. [8], thereby adversely affecting surface finish. This explains the inferior performance of the GC wheel compared to the WA, when grinding under the severest grinding condition ($a_e = 50$ µm), as noted in Fig. 6b. However, noted here is that even for this cutting condition, no evidence of visible grinding burn was observed on the ground surface, as shown in Fig. 7, thus suggesting that the critical temperature for oxide layer formation and phase transformation was not achieved.

With respect to the influence of the radial depth of cut on surface finish, one notes from Fig. 6a that increasing a_e from 10 to 20 µm increased the Ra parameter by 33% on average. Further increases in a_e resulted in similar increases in Ra.

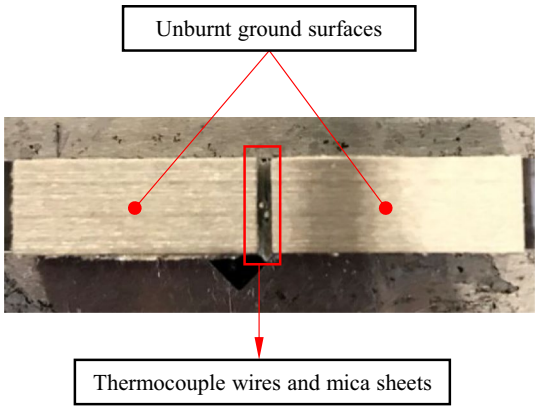

Fig. 7 Ground surface after grinding with the GC wheel and a radial depth of cut (a_e) of 50 µm

Process severity increases with a_e due to higher material removal rates, thereby increasing contact length and abrasive grains penetrating into the workpiece, thereby increasing cutting forces and adversely affecting surface finish. Similar effects regarding surface finish deterioration, when grinding with higher values of depth of cut, was observed by Yao et al. [9] in the grinding of Inconel 718 with alumina and cBN grinding wheels. According to the authors, increasing the depth of cut increases grinding forces, thereby negatively affecting surface roughness of the workpiece.

The average values for the Rz parameter after grinding, as a function of radial depth of cut (a_e), are shown in Fig. 8. From this figure, one notes that the Rz parameter presented similar behavior, as seen with the Ra parameter, except for the highest radial depth of cut ($a_e = 50$ µm) in which both grinding wheels produced similar surface finish, in terms of the Rz parameter on the ground surface. The high values of Rz with lower values of Ra suggest the presence of occasional high peaks and/or deep valleys on those surfaces ground after grinding with this specific condition (WA grinding wheel and $a_e = 50$ µm). This result may be due to the WA abrasive wear of the grain on the mechanism, which holds the distinct possibility of producing a complete break-out or macro-fracture instead of micro-fracture, due to its high fracture toughness or low friability in comparison with GC abrasive grains [14]. In this sense, due to the high cutting forces required for grinding Inconel 718 with high values of radial depth of cut (a_e), WA abrasive grains break-out, thereby increasing empty spaces on the cutting area of the grinding wheel, which may contribute to increasing the difference in height between peaks and valleys on ground surfaces, thus reflecting a higher Rz parameter.

The ANOVA results and graphs for main effects and interactions are shown in Table 7 and in Fig. 9, respectively. Similar to that obtained for the Ra parameter, all factors were statistically significant concerning the Rz

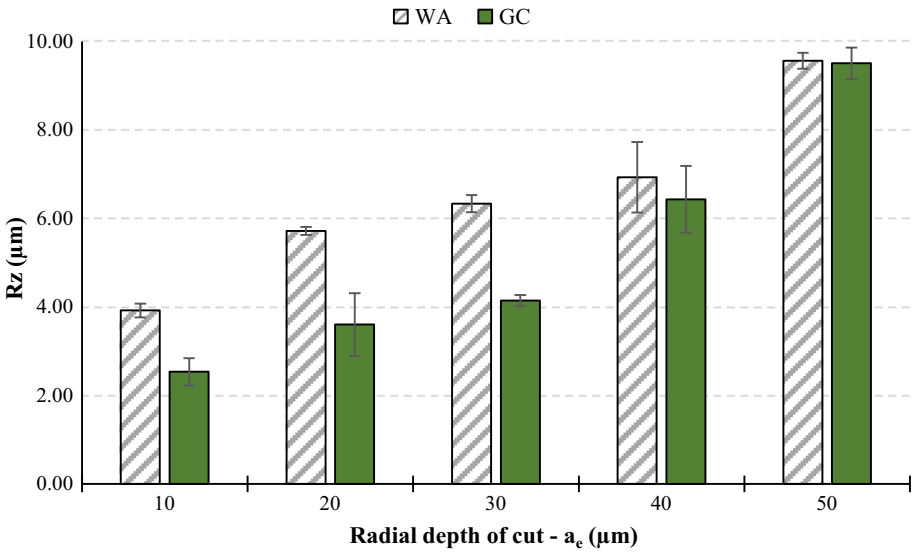

Fig. 8 Roughness Rz of Inconel 718, after grinding with WA and GC grinding wheels, as a function of radial depth of cut (a_e)

Table 7 Analysis of variance (ANOVA) for Rz parameter results

Source	DoF	SS	MS	*F*-value	*P*-value
Main effects					
(1) Abrasive type	1	11.719	11.7187	57.14	0.000
(2) a_e (µm)	4	137.746	34.4364	167.90	0.000
2-Factor interaction					
(1) * (2) Abrasive type vs. a_e (µm)	4	5.455	1.3639	6.65	0.001
Error	20	4.102	0.2051		
Total	29	159.022			

parameter results, including those obtained for abrasive type and a_e interaction. Furthermore, the main effects and interaction graphs show similar trends, indicating that the GC grinding wheel is more suited for grinding Inconel 718 (under the tested conditions) in comparison with WA, especially for low values of radial depth of cut (a_e).

3.2 Cutting region temperature

The cutting region temperatures measured during the grinding experiments as a function of radial depth of cut (a_e), for both abrasive types tested in this work, are shown in Fig. 10. From this figure one notes that the lowest temperature of about 255 °C was recorded during grinding with WA wheels and the lowest depth of cut ($a_e = 10$ µm), whereas the highest value of 1114 °C was recorded when grinding with the GC grinding wheel, with the highest depth of cut ($a_e = 50$ µm). Grinding with the GC grinding wheel generated higher cutting temperatures when compared to WA grinding wheels, regardless the depth of cut employed. Furthermore, one notes from Fig. 10 that the higher the radial depth of cut, the higher the cutting region temperature, which is the same tendency observed with the surface roughness results (Figs. 5 and 8).

The ANOVA results for temperature measurements are shown in Table 8. Noted here is that both factors (abrasive type and radial depth of cut) were statistically significant to cutting region temperature (*P*-value < 0.050). However, the interaction between abrasive type and a_e presented a high *P*-value (0.900), unlike surface finish results. Therefore, the

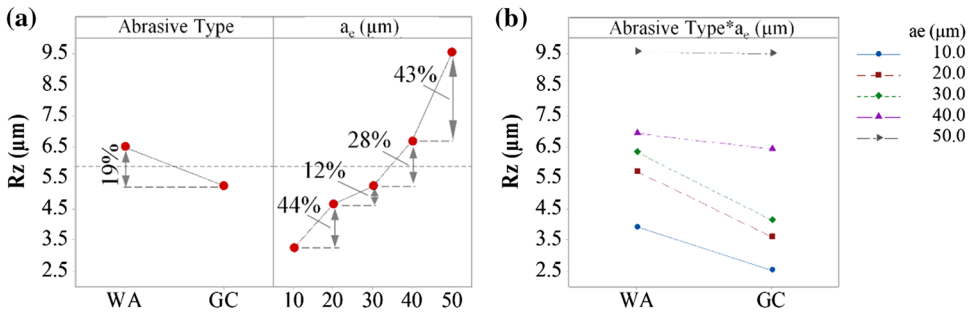

Fig. 9 Main effects and interaction graphs for Rz parameter results

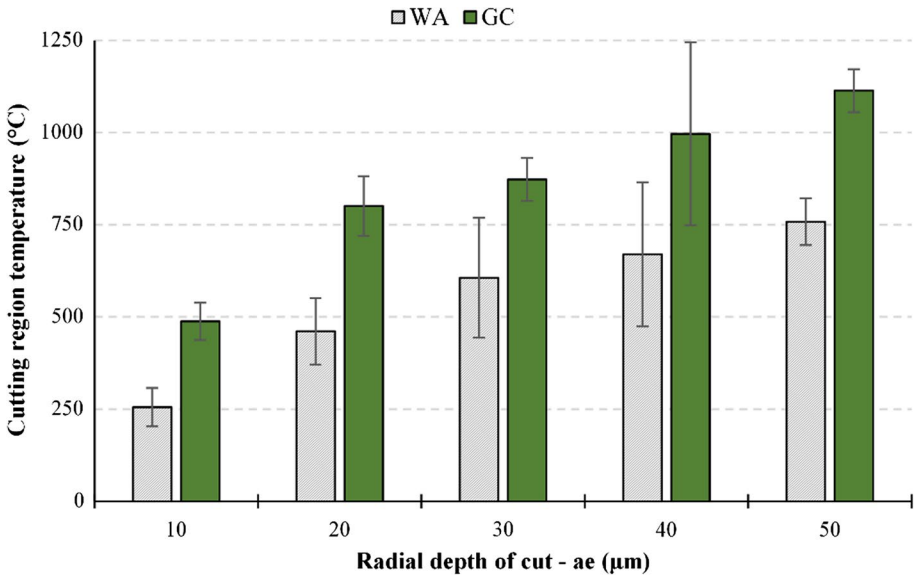

Fig. 10 Cutting region temperature, as a function of radial depth of cut (a_e)

Table 8 Analysis of variance (ANOVA) for cutting region temperature results

Source	DoF	SS	MS	*F*-value	*P*-value
Main effects					
(1) Abrasive type	1	695,250	695,250	44.31	0.000
(2) a_e (µm)	4	1,126,438	281,609	17.95	0.000
2-Factor interaction					
(1) * (2) Abrasive type vs. a_e (µm)	4	16,319	4080	0.26	0.900
Error	20	313,839	15,692		
Total	29	2,151,845			

interaction between the factors was not statistically significant for temperature results considering a confidence interval of 95%. Main effects and interaction graphs for cutting region temperature results are shown in Fig. 11.

From Fig. 11a, grinding with WA wheels is noted as contributing toward a reduction in cutting region temperature by 55%, in general, when compared to GC grinding wheels. The higher temperatures at the cutting zone, during grinding with the GC wheel, is due to the higher friction generated at the contact zone, which is a result of GC the abrasive wear of the grain on the mechanism. In light of its high friability, GC abrasive grits tend to present micro-fracture and wear flat [14], which contributes in a big way toward rubbing, thereby increasing heat generation and temperature during grinding. According to Jackson and Davim [14], as the cutting region temperature increases, the wear mechanism of the abrasive goes from macro- to micro-fracture and then to wear flat formation, which contributes to further temperature increases. This corroborates to the higher values of surface roughness (Ra parameter) observed after grinding with the GC under the worst case condition ($a_e = 50$ µm), since the temperature was higher when using this abrasive and, as such could lead to wear flat formation.

Worthy of mention here is that comparing the temperature results (Fig. 10) with those of roughness (Fig. 5), although the temperature reached, during grinding with the GC wheel, was higher in comparison with WA for all conditions tested, at relatively low levels this higher temperature was not sufficient to favor material adhesion or abrasive wear flat, which consequently deteriorated surface finishing. However, for the worst case conditions ($a_e = 40$ µm and 50 µm), in which higher temperatures were reached (over 1000 °C), one notes

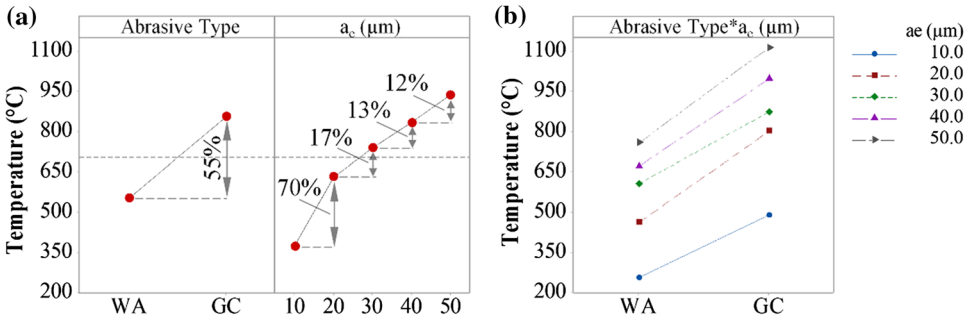

Fig. 11 Main effects and interaction graphs for cutting region temperature results

from Fig. 5 that the surface roughness tended to get worse, when compared with the result obtained after grinding with WA.

The corroborator Tso [28] studied the chip geometry in the grinding of Inconel 718 with different types of grinding wheels (WA, GC and cBN) and noted a peculiar type of chip when grinding with the GC wheel, named as "ripping chip." The occurrence of this type of chip was attributed by the author to the development of high grinding temperatures at the contact zone, as a result of intense attrition wear experienced by the GC abrasive grains. In this context, the higher cutting region temperatures recorded when grinding with the GC grinding wheel in comparison with WA, as shown in Figs. 10 and 11a, corroborates with the findings of Tso [28].

Regarding radial depth of cut (a_e), one notes from Fig. 11a that the cutting region temperatures increased with a_e, as already mentioned. However, its increase was particularly higher (70%) when a_e increased from 10 to 20 µm. Further increases in a_e also increased the cutting region temperatures, but to a lesser degree. Higher values of radial depth of cut increases the contact area between abrasive grain and workpiece, thereby increasing the required grinding forces to promote plastic deformation and workpiece material shearing. Consequently, the grinding power is increased, which results in greater heat generation at the contact zone, thereby increasing the cutting region temperature. Similar results of grinding temperature increase with radial depth of cut were observed by Li et al. [40] in the grinding of Inconel 718 with cBN grinding wheels, and by Chen et al. [41] in grinding Inconel 718 with cBN grinding wheels, while using an optimized cooling–lubrication technique.

A noteworthy observation from Fig. 11b is that the cutting region temperature, as a function of abrasive type, showed similar behavior according to the variation in the radial depth of cut (a_e), resulting in interaction graphs with near parallel curves. This behavior is a consequence of low statistical significance of the interactions, as shown in Table 8 (P-value equal to 0.9).

4 Conclusions

After performing grinding experiments of Inconel 718 with the two conventional abrasive grit types (white aluminum oxide—WA and green silicon carbide—GC) and cutting fluid applied via conventional technique (wet grinding), the following conclusions can be drawn:

- Grinding Inconel 718 with the GC wheel contributed to improved surface finish in comparison with the use of the WA wheel. In general, a 14% and 19% reduction were observed for Ra and Rz, respectively.
- The use of GC grinding wheels promoted, in general, the development of cutting region temperatures 55% higher in comparison with grinding with the WA wheel.
- Comparing the two conventional abrasives types (WA and GC), in terms of surface roughness, the GC is more suitable for grinding Inconel 718 with conventional cutting fluid application (wet grinding), even though it presents higher cutting region temperatures. However, emphasis is here placed on the fact that for high material removal rates (e.g., higher values of radial depth of cut), the higher attrition wear of the GC abrasive grits contributes to further increases in temperature at the contact zone, thereby generating a slightly rougher ground surface in comparison with WA wheel.

Acknowledgement The authors would like to thank the Post Graduate Program of Mechanical Engineering and Multiuser Laboratory of Chemistry Institute at UFU and the Conselho Nacional de Desenvolvimento Científico e Tecnológico (CNPq) for technical and financial support. Finally, the authors would also like to thank the Saint-Gobain Abrasives, Villares Metals S.A and Blaser Swisslube Brazil for the supplying of the tools, workpiece material and coolant used, respectively, in this work.

Author contributions R. Ruzzi performed the experiments, analysis of results and manuscript writings; R. de Paiva contributed to the experimentation, analysis results and manuscript writings; A. Machado overviewed the whole process and supported the discussion of the results; R. da Silva proposed the work topic and helped with results analysis.

Funding This study was partly funded by the Conselho Nacional de Desenvolvimento Científico e Tecnológico (CNPq)—grant references 141472/2017-0 and 426018/2018-4.

Declarations

Conflict of interest The authors declare that there is no conflict of interest regarding the publication of this paper.

Ethical approval This study complies with the ethical standards set out by Springer.

References

1. Dudzinski D, Devillez A, Moufki A et al (2004) A review of developments towards dry and high speed machining of Inconel 718 alloy. Int J Mach Tools Manuf 44:439–456. https://doi.org/10.1016/S0890-6955(03)00159-7
2. Mahata S, Kundu A, Mukhopadhyay M et al (2018) Exploring grind ability of Inconel 718 using small quantity cooling and lubrication technique. Mater Today Proc 5:4523–4530. https://doi.org/10.1016/j.matpr.2017.12.022
3. Klocke F, Soo SL, Karpuschewski B et al (2015) Abrasive machining of advanced aerospace alloys and composites. CIRP Ann Manuf Technol 64:581–604. https://doi.org/10.1016/j.cirp.2015.05.004

4. Loria EA 140 Recent Developments in the Progress of Superalloy 718 رد اهتفرشیپ .pdf. 33–36
5. Choudhury I, El-Baradie M (1998) Machinability of nickel-base super alloys: a general review. J Mater Process Technol 77:278–284. https://doi.org/10.1016/S0924-0136(97)00429-9
6. Ezugwu EO, Bonney J, Yamane Y (2003) An overview of the machinability of aeroengine alloys. J Mater Process Technol 134:233–253. https://doi.org/10.1016/S0924-0136(02)01042-7
7. De Oliveira D, De Paiva RL, da Silva RB, de Carvalho Castro PH (2020) Assessment of the grindability of Inconel 718 under different coolant delivery techniques. J Braz Soc Mech Sci Eng 42:20. https://doi.org/10.1007/s40430-019-2093-0
8. Sinha MK, Setti D, Ghosh S, Venkateswara Rao P (2016) An investigation on surface burn during grinding of Inconel 718. J Manuf Process 21:124–133. https://doi.org/10.1016/j.jmapro.2015.12.004
9. Yao CF, Jin QC, Huang XC et al (2013) Research on surface integrity of grinding Inconel718. Int J Adv Manuf Technol 65:1019–1030. https://doi.org/10.1007/s00170-012-4236-7
10. Sinha MK, Madarkar R, Ghosh S, Paruchuri VR (2019) Some investigations in grindability improvement of Inconel 718 under ecological grinding. Proc Inst Mech Eng Part B J Eng Manuf 233:727–744. https://doi.org/10.1177/0954405417752513
11. Xi X, Ding W, Wu Z, Anggei L (2020) Performance evaluation of creep feed grinding of γ-TiAl intermetallics with electroplated diamond wheels. Chin J Aeronaut. https://doi.org/10.1016/j.cja.2020.04.031
12. Hadad MJ, Tawakoli T, Sadeghi MH, Sadeghi B (2012) Temperature and energy partition in minimum quantity lubrication-MQL grinding process. Int J Mach Tools Manuf 54–55:10–17. https://doi.org/10.1016/j.ijmachtools.2011.11.010
13. Marinescu I, Hitchiner M, Uhlmann E (2006) Handbook of machining with grinding wheels
14. Jackson MJ, Davim JP (2011) Machining with abrasives. Springer US, Boston
15. Cao Y, Zhu Y, Ding W et al (2021) Vibration coupling effects and machining behavior of ultrasonic vibration plate device for creep-feed grinding of Inconel 718 nickel-based superalloy. Chin J Aeronaut. https://doi.org/10.1016/j.cja.2020.12.039
16. Sinha MK, Madarkar R, Ghosh S, Rao PV (2017) Application of eco-friendly nanofluids during grinding of Inconel 718 through small quantity lubrication. J Clean Prod 141:1359–1375. https://doi.org/10.1016/j.jclepro.2016.09.212
17. de Souza RR, Lima de Paiva R, Gelamo RV et al (2021) Study on grinding of Inconel 625 and 718 alloys with cutting fluid enriched with Multilayer Graphene Platelets. Wear. https://doi.org/10.1016/j.wear.2021.203697
18. Klocke F (2009) Manufacturing processes 2. Springer, Berlin
19. Marinescu ID, Rowe WB, Dimitrov B, Inasaki I (2004) Abrasives and abrasive tools. Tribol Abras Mach Process. https://doi.org/10.1016/b978-081551490-9.50012-8
20. Rowe WB (2013) Principles of modern grinding technology, 2nd edn. William Andrew
21. Ashby MF, Jones DRH (2005) Engineering materials 1: an introduction to mictrostructures. Process Des
22. Barsoum MW (2002) Fundamentals of ceramics. Fundam Ceram. https://doi.org/10.1887/0750309024
23. Li BK, Miao Q, Li M et al (2020) An investigation on machined surface quality and tool wear during creep feed grinding of powder metallurgy nickel-based superalloy FGH96 with alumina abrasive wheels. Adv Manuf 8:160–176. https://doi.org/10.1007/s40436-020-00305-2
24. Huddedar S, Chitalkar P, Chavan A, Pawade RS (2012) Effect of cooling environment on grinding performance of nickel based superalloy Inconel 718. J Appl Sci 12:947–954. https://doi.org/10.3923/jas.2012.947.954
25. Tawakoli T, Hadad MJ, Sadeghi MH et al (2009) An experimental investigation of the effects of workpiece and grinding parameters on minimum quantity lubrication—MQL grinding. Int J Mach Tools Manuf 49:924–932. https://doi.org/10.1016/j.ijmachtools.2009.06.015
26. De Oliveira D, Da Silva RB, Gelamo RV (2019) Influence of multilayer graphene platelet concentration dispersed in semi-synthetic oil on the grinding performance of Inconel 718 alloy under various machining conditions. Wear 426–427:1371–1383. https://doi.org/10.1016/j.wear.2019.01.114
27. Tso P-L (1995) Study on the grinding of Inconel 718. J Mater Process Tech 55:421–426. https://doi.org/10.1016/0924-0136(95)02026-8
28. Tso P-L (1995) An investigation of chip types in grinding. J Mater Process Technol 53:521–532. https://doi.org/10.1016/0924-0136(94)01746-N
29. Kuriyagawa T, Syoji K, Ohshita H (2003) Grinding temperature within contact arc between wheel and workpiece in high-efficiency grinding of ultrahard cutting tool materials. J Mater Process Technol 136:39–47
30. Batako AD, Rowe WB, Morgan MN (2005) Temperature measurement in high efficiency deep grinding. Int J Mach Tools Manuf 45:1231–1245. https://doi.org/10.1016/j.ijmachtools.2005.01.013
31. Awale AS, Vashista M, Khan Yusufzai MZ (2020) Multi-objective optimization of MQL mist parameters for eco-friendly grinding. J Manuf Process 56:75–86. https://doi.org/10.1016/j.jmapro.2020.04.069
32. Thellaputta GR, Chandra PS, Rao CSP (2017) Machinability of nickel based superalloys: a review. Mater Today Proc 4:3712–3721. https://doi.org/10.1016/j.matpr.2017.02.266
33. Filho AF, da Silva LRR, de Souza RR et al (2019) Influence of milling direction in the machinability of Inconel 718 with submicron grain cemented carbide tools. Int J Adv Manuf Technol 105:1343–1355. https://doi.org/10.1007/s00170-019-04328-3
34. Li HZ, Zeng H, Chen XQ (2006) An experimental study of tool wear and cutting force variation in the end milling of Inconel 718 with coated carbide inserts. J Mater Process Technol 180:296–304. https://doi.org/10.1016/j.jmatprotec.2006.07.009
35. Special Metals (2008) Product handbook of high-performance alloys. Special Metals Corporation
36. Bradley EF (1988) Superalloys; a technical guide. ASM International, Metals Park
37. de Souza RR, Lima de Paiva R, Ribeiro da Silva LR et al (2021) Comprehensive study on Inconel 718 surface topography after grinding. Tribol Int 158:106919. https://doi.org/10.1016/j.triboint.2021.106919
38. ISO 4288:1996 (1996) Geometrical Product Specifications (GPS)—Surface texture: profile method—rules and procedures for the assessment of surface texture. 8
39. Kalpakjian S, Schmid SR (2008) Manufactura, ingeniería y Tecnología, 5th edn. Pearson Prentice Hall, México
40. Li Z, Ding W-F, Ma C-Y, Xu J-H (2015) Grinding temperature and wheel wear of porous metal-bonded cubic boron nitride superabrasive wheels in high-efficiency deep grinding. Proc Inst Mech Eng Part B J Eng Manuf. https://doi.org/10.1177/0954405415617928
41. Chen ZZ, Xu JH, Ding WF et al (2015) Grinding temperature during high-efficiency grinding Inconel 718 using porous CBN wheel with multilayer defined grain distribution. Int J Adv Manuf Technol 77:165–172. https://doi.org/10.1007/s00170-014-6403-5

Publisher's Note Springer Nature remains neutral with regard to jurisdictional claims in published maps and institutional affiliations.